Astron. Astrophys. 324, 1211–1221 (1997)

ASTRONOMY
AND
ASTROPHYSICS

Polarization of the hydrogen H_α line in solar flares: contribution of the different radiative and collisional processes

E. Vogt[1], **S. Sahal-Bréchot**[2], **and J.C. Hénoux**[3]

[1] Observatoire de Paris-Meudon, DASOP, CNRS URA 2080 (Laboratoire de Physique du Soleil et de l'Héliosphère), 5, place Jules Janssen, F-92195 Meudon Cedex, France (Etienne.Vogt@obspm.fr)
[2] Observatoire de Paris-Meudon, DAMAp, CNRS URA 812 (Laboratoire Atomes et Molécules en Astrophysique), 5, place Jules Janssen, F-92195 Meudon Cedex, France (Sylvie.Sahal-Brechot@obspm.fr)
[3] Observatoire de Paris-Meudon, DASOP, CNRS URA 2080 (Laboratoire de Physique du Soleil et de l'Héliosphère), 5, place Jules Janssen, F-92195 Meudon Cedex, France (Jean-claude.Henoux@obspm.fr)

Received 30 May 1996 / Accepted 19 February 1997

Abstract. Linear polarization of the H_α line of hydrogen has been observed in solar flares. The observed polarization degree can be as high as 10 % for a flare located near the limb and a one minute integration time. This polarization is currently explained as anisotropic collisional excitation of the n = 3 level by vertical beams of protons with an energy greater than a few keV. Transfer of population between the Zeeman excited states by the local protons with an isotropic velocity distribution may reduce the polarization expected from the beam bombardment only. The amplitude of this effect has been computed by solving the statistical equilibrium equations for a 9-level hydrogen atom (all the levels of $n = 1, 2, 3$ including fine structure) for three different atmospheric models. The different collisional and radiative processes for populating and depopulating the Zeeman sublevels have been taken into account: excitation and deexcitation by collisions with the protons of the beam and with the local electrons and protons, excitation by the local Ly_α, Ly_β and H_α radiation, and deexcitation by spontaneous emission. It has been found that the polarization is not destroyed but reduced by a factor two to ten. Beams of non-thermal particles can be, as assumed previously, at the origin of the observed polarization, however, to get a significant degree of polarization, the flux of these particles must be significantly higher than that originally expected.

Key words: atomic processes – line: formation – polarization – Sun: flares

1. Introduction

Linear polarization of the H_α line of hydrogen has been observed in solar flares (Hénoux et al. 1990; Vogt 1992; Vogt and Hénoux 1995). The observed polarization degree can be as high as 10 % for a flare located near the limb and a one minute integration time. This polarization can be explained as anisotropic collisional excitation of the n = 3 level by vertical beams of protons with an initial energy at the coronal level of a few hundred keV. A quantitative study of the observed polarization should allow the determination of the characteristics of these energetic particles and the role they play in the flaring phenomenon. For that, we need to solve the statistical equilibrium equations which give us the levels populations, taking into account all the processes acting on the atomic levels populations and in particular, the transitions between Zeeman sublevels induced by collisions with the protons and electrons of the flaring medium. Studies made of the polarization of the H_α and H_β lines in solar prominences showed that these collisions have a significant depolarizing effect (Bommier et al. 1986, 1994), in spite of a density (of the order of 10^{10} cm^{-3}) lower than the one present in a flaring atmosphere. It is thus necessary to study the influence of the collisions with the thermal particles on the polarization of the emitted radiation. In particular, we will consider the effects of a potential anisotropy of the velocity distribution of the protons of the medium.

The computation of the characteristics of collisional anisotropic processes has been done in a former paper (Sahal-Bréchot et al. 1996). Here, we will use these results to solve the statistical equilibrium equations, then we will analyse the results obtained. But first, we present and evaluate the physical parameters taken into consideration.

2. Starting hypothesis

Firstly, the structure of the solar atmosphere (temperature and density versus altitude) is described by semi-empirical atmosphere models built in a way suited to reproduce different observed line profiles. Three models are used: the first one is the average quiet atmosphere model *VAL C* (Vernezza et al. 1981),

Send offprint requests to: E. Vogt

the second is the hotter plage model *VAL F*, and the last one is the flaring atmosphere model *F1* (Machado et al. 1980).

We assume that the atmosphere is bombarded by a vertical beam of energetic directed protons with a differential particle number flux given by the usual power law at their injection site in the corona

$$\frac{dN}{dE_i}(E_i) \times v(E_i) \;=\; K E_i^{-\delta} \quad , \quad E_i \geq E_{i0} \tag{1}$$

where $\frac{dN}{dE_i}$ is the density of protons of energy E_i at injection per energy band dE_i and $v(E_i)$ is the proton velocity. E_{i0} is the minimum energy required for the proton to reach the chromospheric H_α forming layers. The δ exponent is assigned the value 4.

The proton number flux conservation condition

$$\frac{dN}{dE_i}(E_i) \times v(E_i)\, dE_i \;=\; \frac{dN}{dE} \times v(E)\, dE \tag{2}$$

relates the proton number fluxes at coronal and chromospheric layers. Consequently, the total particle number and energy fluxes $\mathscr{F}$ and $\mathscr{E}$ are given respectively (Emslie 1978; Chambe and Hénoux 1979; Hénoux et al. 1990) by

$$\mathscr{F} \;=\; K \int_{E_{i0}}^{\infty} E_i^{-\delta} dE_i \;=\; K \frac{E_{i0}^{-(\delta-1)}}{\delta - 1} \tag{3}$$

$$\mathscr{E} \;=\; K \int_{E_{i0}}^{\infty} E_i^{-(\delta-1)} dE_i \;=\; K \frac{E_{i0}^{-(\delta-2)}}{\delta - 2} \;=\; \mathscr{F} \times \frac{\delta - 1}{\delta - 2} E_{i0} \tag{4}$$

Estimations of the non thermal effects were made assuming the same particle number flux $\mathscr{F}$ for the three atmospheric models ($5\ 10^{14}$ cm^{-2}.s^{-1} $\leq \mathscr{F} \leq$ $5\ 10^{17}$ cm^{-2}.s^{-1}). Since the minimum energies E_{i0} required for a proton to reach the H_α forming layers are respectively 100 and 200 keV for models *VAL C* and *F1*, we will use the average value of 150 keV for E_{i0} in all 3 models. Thus, the proton energy fluxes associated with the particle number fluxes used are $1.8\ 10^8$ ergs.cm^{-2}.s^{-1} $\leq \mathscr{E} \leq$ $1.8\ 10^{11}$ ergs.cm^{-2}.s^{-1}.

As we are concerned with charged particles of the flaring medium, we consider two different cases: The first with an isotropic velocity distribution due to thermal agitation and the second with an anisotropic velocity distribution where a drift motion in the horizontal plane is added to thermal agitation (Sahal-Bréchot et al. 1996). A model liable to produce such an anisotropy of the protons of the medium during the impulsive phase of flares has been recently proposed (Emslie and Hénoux 1995).

Then, we suppose that the magnetic field is directed along the vertical, like the directed beam, so that the studied system has a cylindrical symmetry around the vertical axis that simplifies the calculations; and that its intensity is not too high, so that we can neglect the Zeeman splitting. Level crossings start to become important for a field strength of the order of $10^3 G$, which is higher than the typical field in a chromospheric flare (of the order of a few $10^2 G$). However, there is an observation where a strong magnetic field (of the order of $750G$) has been found in chromospheric flare kernels from slit spectra of the He 10380 line taken at the NSO VTT (Penn and Kuhn 1995). So it may be justified to take Zeeman splitting into account in a later continuation of this work. This would presumably slightly enhance the resulting polarization.

An hydrogen atom with 3 main levels $n = 1, n = 2$ and $n = 3$, and their orbital levels $l = 0, \ldots, n-1$ is considered. We have verified by numerical computations that the transitions with the continuum (ionisation and recombination) do not significantly affect the polarization, so we can neglect them. We will again treat two different cases according to whether or not we neglect the fine structure (splitting between $j = l - 1/2$ and $j = l + 1/2$ levels). In the case with fine structure splitting, we suppose that the j levels of the excited states are completely separated; in other words, that their width is lower than their energy separation. This is true as long as the density of the medium protons and electrons is lower than 10^{13} cm^{-3}. As for the hyperfine structure, it is completely degenerate and can be ignored (Bommier and Sahal 1982). We expect the H_α polarization to be reduced in the fine structure case as only 4 out of 7 components of the line may be polarized; whereas without fine structure, 2 out of 3 components may carry polarization. The case without fine structure may still have some physical reality in situations where the background particles density or the magnetic field are very high and cause the fine structure levels to mix.

Finally, we neglect radiative transfer and suppose that the incident radiation is isotropic and unpolarized. Using the last diffusion approximation (Stenflo 1982), we calculate the H_α line polarization at its unity optical depth level in the flaring atmosphere. Our goal is the calculation of the linear polarization degree τ of the H_α line which is expressed as a function of the Stokes parameters I, Q and U by:

$$\tau = \frac{\sqrt{Q^2 + U^2}}{I} \tag{5}$$

The Stokes parameters themselves are expressed as functions of elements of the atomic density matrix.

3. The statistical equilibrium equations

Our goal is to determine the density matrix of the hydrogen atom previously described. In a steady state and owing to the cylindrical symmetry, this density matrix only contains diagonal elements which are the populations N_i of the sublevels i. The system of statistical equilibrium equations is then written for each sublevel $i = n_i l_i j_i m_i$ as:

$$N_i \sum_{k \neq i} P_{i \to k} = \sum_{k \neq i} N_k P_{k \to i} \tag{6}$$

where the $P_{k\to i}$ are the total transition probabilities between sublevels (sum of radiative and collisional contributions). We can also rewrite these equations as:

$$\sum_k N_k P_{k\to i} = 0 \tag{7}$$

introducing relaxation terms:

$$P_{i\to i} = -\sum_{k\neq i} P_{i\to k} \tag{8}$$

To close the system, one generally replace one of the equations — they are not linearly independant — by the normalisation condition:

$$\sum_i N_i = N_H \tag{9}$$

where N_H is the total density of neutral hydrogen in the flaring atmosphere.

3.1. Irreducible tensorial operators

Owing to the cylindrical symmetry of the problem, we will greatly simplify the equations by using a development of the atomic density matrix on the basis of the irreducible tensorial operators T^k_q. This basis is particularly suited to the study of rotationally invariant processes as the T^k_q follow the transformation laws of the spherical harmonics (Fano 1949, 1954, 1957; Blum 1981).

The multipolar expansion elements[1] of the density matrix ${}^{nljn'l'j'}\rho^k_q$ with $q \neq 0$ are zero owing to the cylindrical symmetry (magnetic field and directed beam are both along the vertical). Further, as we made the hypothesis that the different energy levels are well separated, coherence terms between levels ${}^{nljn'l'j'}\rho^k_0$ with $(nlj) \neq (n'l'j')$ are also zero. Therefore, there are only ${}^{nlj}\rho^k_0$ terms left which can be written in terms of the Zeeman sublevels populations N_{nljm} as (Sahal-Bréchot 1977):

$${}^{nlj}\rho^k_0 = \sum_m (-1)^{j-m}\sqrt{2k+1}\begin{pmatrix} j & k & j \\ -m & 0 & m \end{pmatrix} N_{nljm} \tag{10}$$

where the entity in parenthesis is a so-called *"3j"* coefficient.

In addition, the reflection symmetry relative to the plane perpendicular to the magnetic field implies that terms of odd k rank are zero ($N_{nljm} = N_{nlj-m}$). Therefore, we only need multipolar terms of rank 0 (population) and 2 (alignment) to calculate the linear polarization. There are also terms of rank 4 for the $3d_{5/2}$ level in the statistical equilibrium equations ($k_{max} = 2j$), but they don't appear in the polarization.

We shall then write the statistical equilibrium equations in the basis of the irreducible tensorial operators in the form:

$$\sum_{nljk} \Pi_{nljk\to n'l'j'k'}\,{}^{nlj}\rho^k_0 = 0 \tag{11}$$

[1] One calls *multipolar elements or terms* the elements of the density matrix expressed in the basis of the irreducible tensorial operators

where the $\Pi_{nljk\to n'l'j'k'}$ are the matrix elements of the statistical equilibrium equations expressed in the basis of the irreducible tensorial operators. They are related to the $P_{nljm\to n'l'j'm'}$ by:

$$\begin{aligned}\Pi_{nljk\to n'l'j'k'} &= \sqrt{(2k+1)(2k'+1)} \\ &\times \sum_{mm'} (-1)^{j+j'-m-m'} \begin{pmatrix} j & k & j \\ -m & 0 & m \end{pmatrix} \\ &\begin{pmatrix} j' & k' & j' \\ -m' & 0 & m' \end{pmatrix} P_{nljm\to n'l'j'm'}\end{aligned} \tag{12}$$

The $\Pi_{nljk\to n'l'j'k'}$ divide themselves into two groups. The first contains transition terms between two different nlj levels and are the sum of a radiative contribution $C_{k\to k',nlj\to n'l'j'}$ and a collisional contribution $R_{k\to k',nlj\to n'l'j'}$:

$$\Pi_{nljk\to n'l'j'k'} = C_{k\to k',nlj\to n'l'j'} + R_{k\to k',nlj\to n'l'j'} \tag{13}$$

As for the second, they represent the relaxation of an nlj level and are expressed as a sum of collisional relaxation terms $C^{relax}_{k\to k',nlj\to n'l'j'}$ and radiative relaxation terms $R^{relax}_{k\to k',nlj\to n'l'j'}$ for all the possible ways of relaxation $nlj \to n'l'j'$:

$$\begin{aligned}\Pi_{nljk\to nljk'} &= -\sum_{n'l'j'} C^{relax}_{k\to k',nlj\to n'l'j'} \\ &- \sum_{n'l'j'} R^{relax}_{k\to k',nlj\to n'l'j'}\end{aligned} \tag{14}$$

3.2. Calculation of radiative transition probabilities

The contribution of radiative transitions to the $\Pi_{nljk\to n'l'j'k'}$ takes the form (Sahal-Bréchot 1977):

$$\begin{aligned}R_{k\to k',nlj\to n'l'j'} &= \delta_{kk'} c^{(0)}_{k,j\to j'} \gamma^{(0)}_{nlj\to n'l'j'} \\ &+ c^{(2)}_{k\to k',j\to j'} \gamma^{(2)}_{nlj\to n'l'j'}\end{aligned} \tag{15}$$

Whereas for the relaxation terms which appear in the $\Pi_{nljk\to nljk'}$:

$$\begin{aligned}R^{relax}_{k\to k',nlj\to n'l'j'} &= \delta_{kk'} c^{relax(0)}_{k,j\to j'} \gamma^{(0)}_{nlj\to n'l'j'} \\ &+ c^{relax(2)}_{k\to k',j\to j'} \gamma^{(2)}_{nlj\to n'l'j'}\end{aligned} \tag{16}$$

The $c^{(0)}_{k,j\to j'}$, $c^{(2)}_{k\to k',j\to j'}$, $c^{relax(0)}_{k,j\to j'}$ and $c^{relax(2)}_{k\to k',j\to j'}$ are angular algebra coefficients defined in the previous article (Sahal-Bréchot et al. 1996; see also Sahal-Bréchot 1977).

The $\gamma^{(0)}_{nlj\to n'l'j'}$ represent the radiative emission and absorption probabilities:

$$\gamma^{(0)}_{nlj\to n'l'j'} = \begin{cases} A_{nlj\to n'l'j'} + B_{nlj\to n'l'j'} I_\nu & \text{if } n > n' \\ B_{nlj\to n'l'j'} I_\nu & \text{if } n < n' \end{cases} \tag{17}$$

where $A_{nlj\to n'l'j'}$ and $B_{nlj\to n'l'j'}$ are respectively the Einstein coefficients for spontaneous emission, and absorption or induced emission of the transition considered (but induced emission is most often negligible) and I_ν is the intensity of radiation in the line.

The $\gamma^{(2)}_{nlj\to n'l'j'}$ represent the alignment creation induced by radiative processes. They are zero since we suppose that the incident radiation is isotropic and non-polarized. The case of an anisotropic or polarized incident radiation will be treated in a subsequent paper.

The intensity of incident radiation (integrated over line profile and directions) is obtained by numerical computations of non-polarized radiative transfer (Fang et al. 1993; Hénoux et al. 1993). The program used computes the structure of the flaring atmosphere as a function of altitude, using the initial model (*VAL C*, *VAL F* or *F1*) and the characteristics of the directed proton beam. Here, we are interested in the layer for which the optical depth in the H_α line is closest to unity; this gives us the intensity of radiation in the Ly_α, Ly_β and H_α lines as well as the other physical parameters (temperature, electronic density,...) which we need for our calculations.

3.3. Calculation of collisional transition probabilities

The collisional contribution to the $\Pi_{nljk\to n'l'j'k'}$ is similar to the radiative one if the collisional transitions are treated in the semi-classical perturbation approximation (Sahal-Bréchot et al. 1996):

$$C_{k\to k',nlj\to n'l'j'} = N_P(\delta_{kk'}c^{(0)}_{k,j\to j'}\alpha^{(0)}_{nlj\to n'l'j'} + c^{(2)}_{k\to k',j\to j'}\alpha^{(2)}_{nlj\to n'l'j'}) \quad (18)$$

$$C^{relax}_{k\to k',nlj\to n'l'j'} = N_P(\delta_{kk'}c^{relax(0)}_{k,j\to j'}\alpha^{(0)}_{nlj\to n'l'j'} + c^{relax(2)}_{k\to k',j\to j'}\alpha^{(2)}_{nlj\to n'l'j'}) \quad (19)$$

where N_P is the density of perturbers (protons or electrons), $\alpha^{(0)}_{nlj\to n'l'j'}$ and $\alpha^{(2)}_{nlj\to n'l'j'}$ are respectively the collisional transition rates for population and alignment (cross sections integrated over the perturbers' velocity distribution).

The perturbers considered are the particles of the flaring medium (isotropic electrons, isotropic or anisotropic protons) as well as the energetic protons from the directed beam; we add their respective contributions.

The semi-classical perturbation method described in the preceding article only applies correctly to dipolar electric transitions with $\Delta E_{ij} \ll kT$. For transitions between levels of different n where $\Delta E_{ij} \simeq kT$, the perturbation theory is not expected to give good results, but we use it nevertheless as it allows us to calculate cross sections for all the collisional processes we have to consider. At this time, we do not have more precise data for collisions with protons in transitions between n = 2 and n = 3, and in the fine structure case, we do not have anything else even for electronic collisions; so all the collisional rates used in this work are computed with the semi-classical perturbation method in order to get consistent results between all the different cases.

A comparison with Fritsch and Lin (1983) results for the n = 1 $\to$ n = 2 transitions (or Schöller et al. 1986 for n = 1 $\to$ n = 3) shows that our approximation is acceptable since both results are of the same order of magnitude, the semi-classical perturbation method giving results that are higher by roughly a factor three[2].

For the H_α line polarization, we can expect the $1s \to 3d$ collisional transitions to play a significant role as they are not in competition with radiative transitions. We have no cross section values available for these transitions by collisions with protons and we can not use the semi-classical perturbation method to compute them (they are not dipolar electric transitions). So we have to make an estimation. Looking at the data from Aboudharam et al. (1992) for electronic collisions, we see that the cross section for the $1s \to 3d$ transition is of the order of half of that of the $1s \to 3p$ transition for energies close to the excitation threshold and of the order of one tenth for high energies. Therefore, we assume that the value of the $1s \to 3d$ transition probability by directed protons is also of the order of half of the value obtained for the $1s \to 3p$ transition. This is certainly a very crude estimation but it provides an upper limit to the influence of the $1s \to 3d$ collisional transitions.

3.4. Physical parameters introduced to represent the solar atmosphere

Three differents representations, taken from Vernazza et al. 1981 and Machado et al. 1980, of the thermodynamical state of the solar atmosphere before bombardment by protons were considered; the quiet sun model atmosphere *VAL C*, the model *VAL F* more representative of solar plages and the flaring atmosphere model *F1*. Due to its lower temperature, the *VAL C* model minimizes the effect of the radiation field on the statistical equilibrium equations and will lead to the highest H_α polarization degree. Since flares occur in active regions, the *VAL F* model that represents bright elements in the quiet sun is presumably more appropriate than *VAL C*. The flare model *F1* represents a faint flare as were the flares observed in H_α polarimetry. A numerical radiative transfer code, that takes into account the non-thermal ionization and excitation of hydrogen in an atmosphere bombarded by a proton beam (Fang et al. 1993, Hénoux et al. 1993), was used in order to estimate the Ly_α, Ly_β and H_α line intensities and the atmosphere thermal electron and protons number densities at optical depth unity in H_α.

The rise of the local electron and proton number density which accompanies the rise of the beam proton number flux is due to the non thermal ionization of the atmosphere by these protons. It is worth noticing that non thermal excitation contribute significantly to the formation of the radiation since a proton number flux of the order of 10^{17} cm^{-2}.s^{-1} leads to values of the Ly_β and H_α line intensities similar to those given by the thermal model *F1* ignoring non-thermal effects.

3.5. Solving the statistical equilibrium equations

We are now able to write the statistical equilibrium equations as given by (11). Before solving them, we need to replace one of the equations — we will take the equation for the fundamental

[2] This could lead to an upwards correction of the directed proton fluxes used in this work by half an order of magnitude

Table 1. Input parameters in the case of the quiet model VAL C. This table gives the intensities in Ly_α, Ly_β and H_α (ergs.cm^{-2}.s^{-1}.Hz^{-1}.sr^{-1}), the temperature (K) and the electronic, neutral hydrogen and ionised hydrogen densities (cm^{-3}) at an H_α optical depth of order unity as a function of the directed protons number flux (cm^{-2}.s^{-1}).

$\mathscr{F}$	I_{Ly_α}	I_{Ly_β}	I_{H_α}	T	N_e	N_H	N_{H^+}
5.0 10^{14}	6.66 10^{-10}	8.24 10^{-12}	1.03 10^{-5}	6040	1.79 10^{11}	1.69 10^{13}	1.70 10^{11}
1.4 10^{15}	6.64 10^{-10}	9.18 10^{-12}	1.16 10^{-5}	6040	1.87 10^{11}	1.69 10^{13}	1.77 10^{11}
5.0 10^{15}	6.80 10^{-10}	1.17 10^{-11}	1.44 10^{-5}	6040	2.15 10^{11}	1.69 10^{13}	2.05 10^{11}
1.4 10^{16}	6.99 10^{-10}	1.60 10^{-11}	1.91 10^{-5}	6040	2.67 10^{11}	1.69 10^{13}	2.58 10^{11}
5.0 10^{16}	8.64 10^{-10}	3.96 10^{-11}	3.91 10^{-5}	6040	4.23 10^{11}	1.67 10^{13}	4.15 10^{11}
5.0 10^{17}	5.06 10^{-7}	4.06 10^{-8}	6.83 10^{-5}	6370	6.33 10^{11}	4.15 10^{11}	6.33 10^{11}

Table 2. Input parameters in the case of the hot quiet model VAL F. This table gives the intensities in Ly_α, Ly_β and H_α (ergs.cm^{-2}.s^{-1}.Hz^{-1}.sr^{-1}), the temperature (K) and the electronic, neutral hydrogen and ionised hydrogen densities (cm^{-3}) at an H_α optical depth of order unity as a function of the directed protons number flux (cm^{-2}.s^{-1}).

$\mathscr{F}$	I_{Ly_α}	I_{Ly_β}	I_{H_α}	T	N_e	N_H	N_{H^+}
5.0 10^{14}	2.77 10^{-9}	4.06 10^{-11}	1.23 10^{-5}	6510	2.14 10^{11}	5.51 10^{12}	2.10 10^{11}
1.4 10^{15}	2.77 10^{-9}	4.30 10^{-11}	1.29 10^{-5}	6510	2.26 10^{11}	5.50 10^{12}	2.22 10^{11}
5.0 10^{15}	2.84 10^{-9}	5.35 10^{-11}	1.57 10^{-5}	6510	2.70 10^{11}	5.46 10^{12}	2.66 10^{11}
1.4 10^{16}	3.03 10^{-9}	7.88 10^{-11}	2.17 10^{-5}	6510	3.53 10^{11}	5.37 10^{12}	3.49 10^{11}
5.0 10^{16}	3.75 10^{-9}	1.77 10^{-10}	3.96 10^{-5}	6510	5.61 10^{11}	5.17 10^{12}	5.58 10^{11}
5.0 10^{17}	1.38 10^{-7}	1.40 10^{-8}	8.71 10^{-5}	6740	8.60 10^{11}	6.34 10^{11}	8.60 10^{11}

Table 3. Input parameters in the case of the flare model F1. This table gives the intensities in Ly_α, Ly_β and H_α (ergs.cm^{-2}.s^{-1}.Hz^{-1}.sr^{-1}), the temperature (K) and the electronic, neutral hydrogen and ionised hydrogen densities (cm^{-3}) at an H_α optical depth of order unity as a function of the directed protons number flux (cm^{-2}.s^{-1}).

$\mathscr{F}$	I_{Ly_α}	I_{Ly_β}	I_{H_α}	T	N_e	N_H	N_{H^+}
5.0 10^{14}	1.83 10^{-7}	4.61 10^{-9}	2.12 10^{-5}	8450	1.51 10^{12}	2.84 10^{12}	1.50 10^{12}
5.0 10^{15}	1.83 10^{-7}	4.58 10^{-9}	2.11 10^{-5}	8450	1.51 10^{12}	2.84 10^{12}	1.50 10^{12}
5.0 10^{16}	1.83 10^{-7}	4.77 10^{-9}	2.19 10^{-5}	8450	1.53 10^{12}	2.81 10^{12}	1.53 10^{12}
5.0 10^{17}	1.85 10^{-7}	5.92 10^{-9}	2.67 10^{-5}	8450	1.73 10^{12}	2.61 10^{12}	1.73 10^{12}
1.4 10^{18}	1.97 10^{-7}	7.71 10^{-9}	3.29 10^{-5}	8450	1.98 10^{12}	2.37 10^{12}	1.97 10^{12}
5.0 10^{18}	2.18 10^{-7}	1.32 10^{-8}	5.11 10^{-5}	8450	2.39 10^{12}	1.96 10^{12}	2.38 10^{12}
1.4 10^{19}	3.56 10^{-7}	3.08 10^{-8}	7.40 10^{-5}	8450	2.72 10^{12}	1.63 10^{12}	2.71 10^{12}

level $1s_{1/2}$ — by the normalization condition (9), which we rewrite in the form:

$$\sum_{nlj} \mathscr{N}_{nlj} = 1 \tag{20}$$

introducing the relative populations $\mathscr{N}_{nlj} = N_{nlj}/N_H$.

If we also define the multipolar terms ${}^{nlj}\rho^k_0$ in term of the relative populations, we deduce from Eq. (10) that:

$${}^{nlj}\rho^0_0 = \frac{1}{\sqrt{2j+1}}\,\mathscr{N}_{nlj} \tag{21}$$

From this we get the expression of the normalisation condition in the basis of the irreducible tensorial operators:

$$\sum_{nlj} \sqrt{2j+1}\ {}^{nlj}\rho^0_0 = 1 \tag{22}$$

We are now able to solve the system numerically.

In the case where we account for fine structure splitting, we have a total of 9 levels ($1s_{1/2}$, $2s_{1/2}$, $2p_{1/2}$, $2p_{3/2}$, $3s_{1/2}$, $3p_{1/2}$, $3p_{3/2}$, $3d_{3/2}$ and $3d_{5/2}$) and 14 unknown quantities which are:

- The populations ${}^{nlj}\rho^0_0$ of the 9 levels.
- The alignments ${}^{nlj}\rho^2_0$ of the $2p_{3/2}$, $3p_{3/2}$, $3d_{3/2}$ and $3d_{5/2}$ levels.
- The multipolar term of order 4 ${}^{3d_{5/2}}\rho^4_0$ of the $3d_{5/2}$ level.

In the case without fine structure splitting, the number of levels is reduced to 6 ($1s$, $2s$, $2p$, $3s$, $3p$ and $3d$) and the number of unknown quantities to 10.

The statistical equations were solved for various values of the proton number flux in the vertical energetic proton beam. In order to clearly show the influence of the atmospheric perturbers, the computations were done both with and without including the depolarizing transitions between Zeeman sublevels induced by the collisions with the particles of the medium. When the role of the perturbers was taken into account, two different cases were considered:

- A first one in which the electrons and protons of the medium have both an isotropic thermal velocity distribution.
- A second one where the electrons in the medium have an isotropic velocity distribution function and the protons of

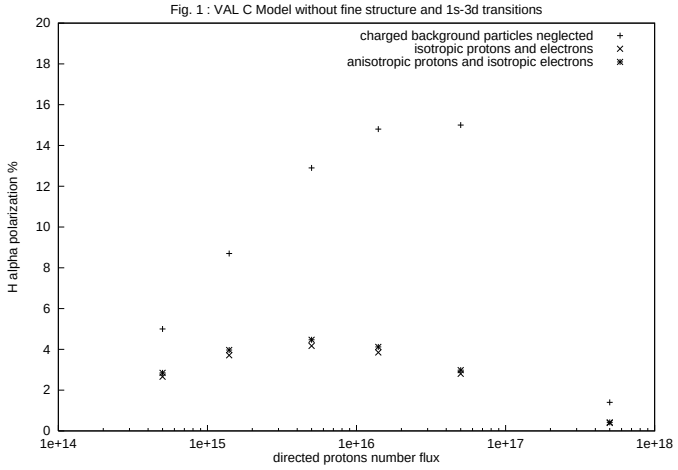

Fig. 1. These figures show the behaviour of the maximum H_α polarization degree τ_{90} (in percent) as a function of the directed proton number flux $\mathscr{F}$ (in $\mathrm{cm}^{-2}.\mathrm{s}^{-1}$) for the three atmospheric models *VAL C*, *VAL F* and *F1*, including or not the effects of fine structure and 1s–3d transitions.

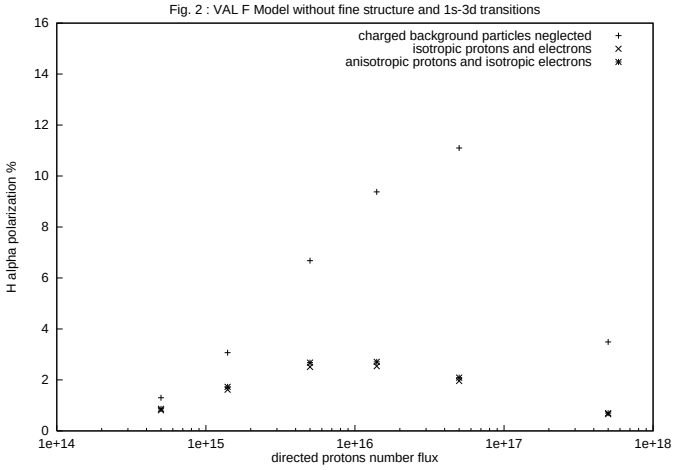

Fig. 2. See Fig. 1

the medium have an horizontal drift velocity close to their thermal speed (drift energy of 0.5 eV).

Once we know the elements of the atomic density matrix, we can use them to calculate the polarization of the emitted radiation.

4. Calculation of the polarization

The polarization degree of the radiation is given by Eq. (5). As the third Stokes parameter U can be zeroed by a judicious choice of reference axis (Sahal-Bréchot 1974b), only I and Q have to be determined. For that, we add the emissivities ϵ_I (respectively ϵ_Q) for each of the transitions who contribute to the line. In the case of H_α, these transitions are: $3p_{1/2} \rightarrow 2s_{1/2}$, $3p_{3/2} \rightarrow 2s_{1/2}$, $3s_{1/2} \rightarrow 2p_{1/2}$, $3s_{1/2} \rightarrow 2p_{3/2}$, $3d_{3/2} \rightarrow 2p_{1/2}$, $3d_{3/2} \rightarrow 2p_{3/2}$ and $3d_{5/2} \rightarrow 2p_{3/2}$ with fine structure splitting and $3p \rightarrow 2s$, $3s \rightarrow 2p$ and $3d \rightarrow 2p$ without fine structure splitting.

The emissivities ϵ_I and ϵ_Q can be written respectively as (Sahal-Bréchot 1977):

$$\epsilon_I(nlj \rightarrow n'l'j') = \frac{h\nu_{nlj\rightarrow n'l'j'}}{4\pi} A_{nlj\rightarrow n'l'j'}(2j+1)(-1)^{j+j'+1} \left(\sqrt{3} \begin{Bmatrix} j & j & 0 \\ 1 & 1 & j' \end{Bmatrix}^{nlj} \rho_0^0 + \frac{\sqrt{3}}{2\sqrt{2}} \begin{Bmatrix} j & j & 2 \\ 1 & 1 & j' \end{Bmatrix}^{nlj} \rho_0^2 (3\cos^2\theta - 1) \right) \quad (23)$$

$$\epsilon_Q(nlj \rightarrow n'l'j') = \frac{h\nu_{nlj\rightarrow n'l'j'}}{4\pi} A_{nlj\rightarrow n'l'j'}(2j+1)(-1)^{j+j'+1} \frac{3\sqrt{3}}{2\sqrt{2}} \begin{Bmatrix} j & j & 2 \\ 1 & 1 & j' \end{Bmatrix}^{nlj} \rho_0^2 \sin^2\theta \quad (24)$$

If we suppose that the frequencies of the different components are equal ($\nu_{nlj\rightarrow n'l'j'} = \nu_{n\rightarrow n'}$), the polarization degree takes the form:

$$\tau_{n\rightarrow n'} = \frac{\sum_{ll'jj'} \epsilon_Q(nlj \rightarrow n'l'j')}{\sum_{ll'jj'} \epsilon_I(nlj \rightarrow n'l'j')} \, . \quad (25)$$

This can be rewritten as:

$$\tau_{n\rightarrow n'} = \frac{3\eta_{n\rightarrow n'} \sin^2\theta}{1 + (3\cos^2\theta - 1)\eta_{n\rightarrow n'}} \, , \quad (26)$$

by defining:

$$\eta_{n\rightarrow n'} = \frac{1}{2\sqrt{2}} \frac{\sum_{ll'jj'}(2j+1)(-1)^{j+j'+1} A_{nlj\rightarrow n'l'j'} \begin{Bmatrix} j & j & 2 \\ 1 & 1 & j' \end{Bmatrix}^{nlj} \rho_0^2}{\sum_{ll'jj'}(2j+1)(-1)^{j+j'+1} A_{nlj\rightarrow n'l'j'} \begin{Bmatrix} j & j & 0 \\ 1 & 1 & j' \end{Bmatrix}^{nlj} \rho_0^0} \, . \quad (27)$$

If we observe at a $\theta = 90$ degrees angle from the magnetic field axis, we get the maximum polarization degree of:

$$\tau_{90}(n \rightarrow n') = \frac{3\eta_{n\rightarrow n'}}{1 - \eta_{n\rightarrow n'}} \, . \quad (28)$$

5. Results and interpretation

The proton number flux dependence of the maximum H_α line polarization τ_{90} that could be observed at 90^o of a proton beam is presented in Figs. 1 to 12. For three different atmospheric models, the polarization was computed without and with fine structure including or not the effects of 1s–3d transitions.

The maximum polarization degree is obtained ignoring fine structure. The polarization degree rises with the proton number flux and saturates when the non-thermal collisional processes dominate over the radiative processes. Exchange of population between sublevels due to collisions with background electrons

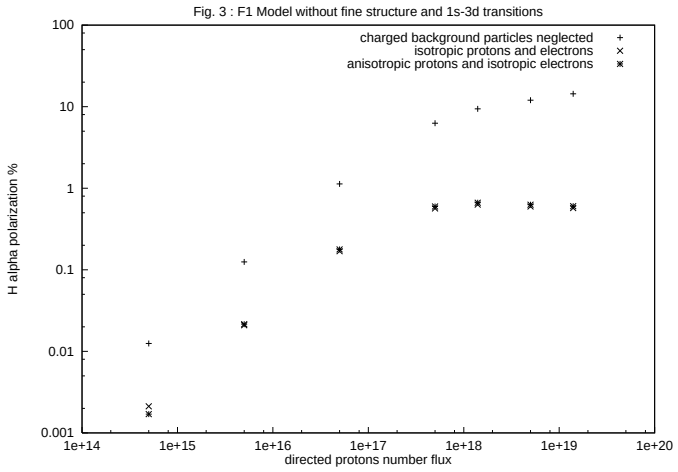

Fig. 3. See Fig. 1

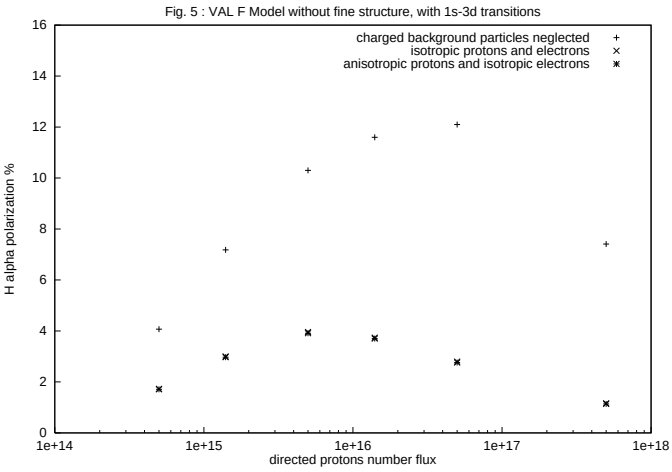

Fig. 5. See Fig. 1

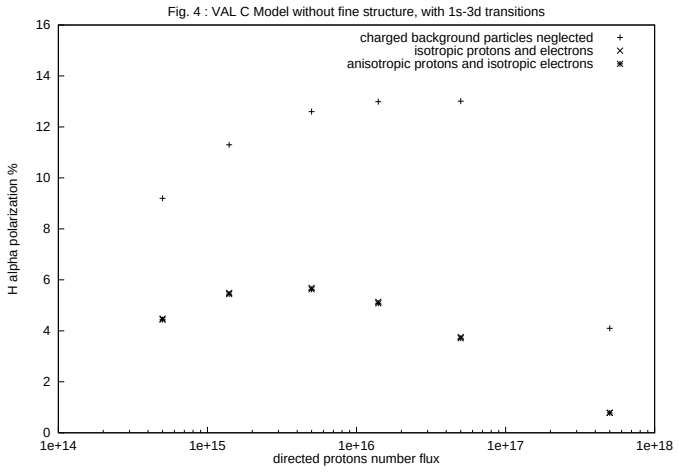

Fig. 4. See Fig. 1

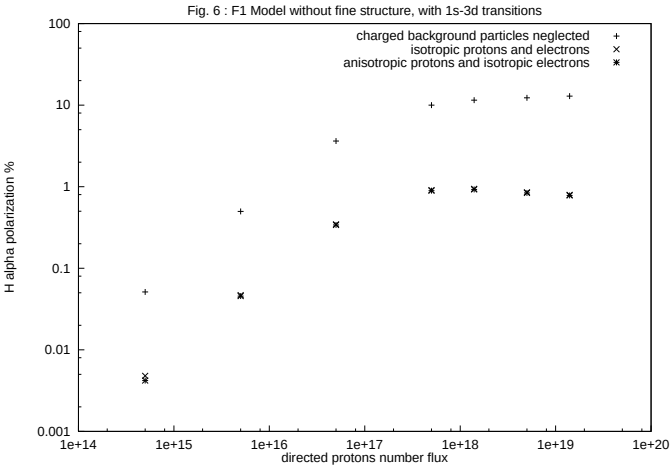

Fig. 6. See Fig. 1

and protons reduces the level of polarization. The increase of the local electron and proton densities that goes with the rise of the proton number flux counterbalances the direct effect on the polarization of the higher proton beam flux. As a result, a maximum of the polarization is reached for some value of the proton number flux. The increase of both the Ly_α, Ly_β and H_α radiation field and the local electron and proton number densities from model *VAL C* to model *F1* leads to a decrease of the expected polarization degree as it can be seen on Fig. 1 to 6. The inclusion of fine structure in the hydrogen atomic model leads to a polarization degree smaller by a factor two to three. Such reduction was expected as the splitting of the levels reduces the number of transitions able to carry alignment relatively to all the possible transitions. This applies to the components of the H_α line and also to the collisional transitions excited by the directed protons. The relative variations of τ_{90} with the beam proton number flux with or without taking into account the depolarizing effect of collisions with background electrons and protons has the same characteristics than in the case without fine structure. Just the level of polarization is reduced when fine structure is taken into account. As in the case without fine structure, the H_α maximum polarization degree τ_{90} decreases from model *VAL C* to model *F1* as can be seen on Figs. 7 to 12.

An anisotropy in the velocity field of background protons slightly modifies the polarization degree when 1s–3d beam-induced transitions are not taken into account. However, a drift energy as high as 1 eV rises the polarization degree by at best a factor 1.3. This could be explained by the fact that excitation and deexcitation balance each other owing to the low energy difference between orbital levels of the hydrogen atom. When 1s–3d transitions are taken into account the effect is even less significant and the polarization degree is indeed reduced.

As to the 1s–3d transitions, their effect on the polarization of H_α is significant since the polarization degree is enhanced by a factor two to four. However, we should remember that these transitions have been introduced in a very approximative way and that their influence and hence the polarization degree is probably overestimated.

One important result provided by our calculations is the confirmation that the transitions between Zeeman sublevels induced

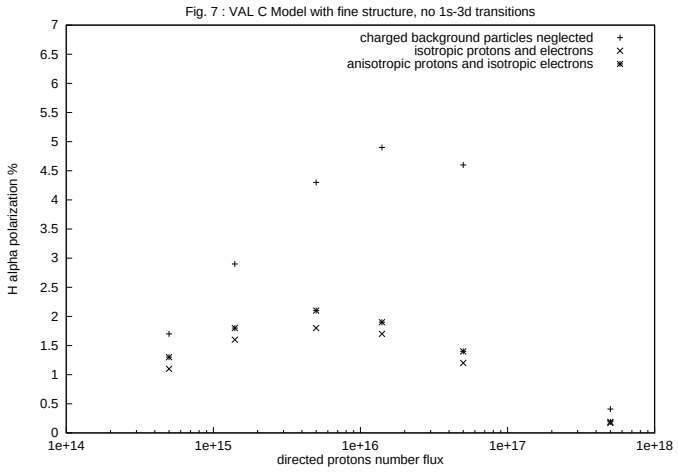

Fig. 7. See Fig. 1

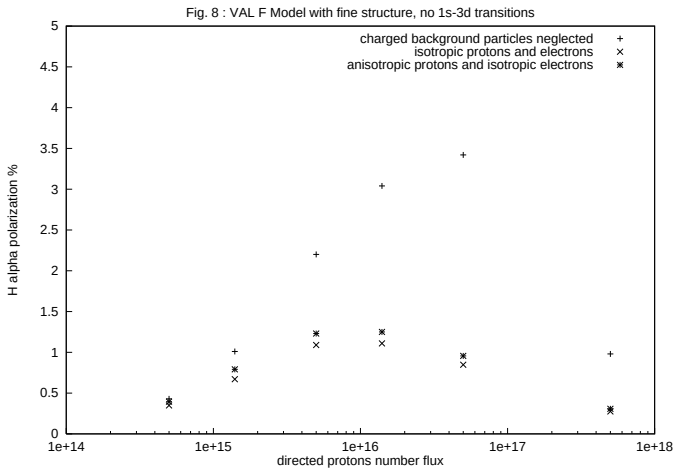

Fig. 8. See Fig. 1

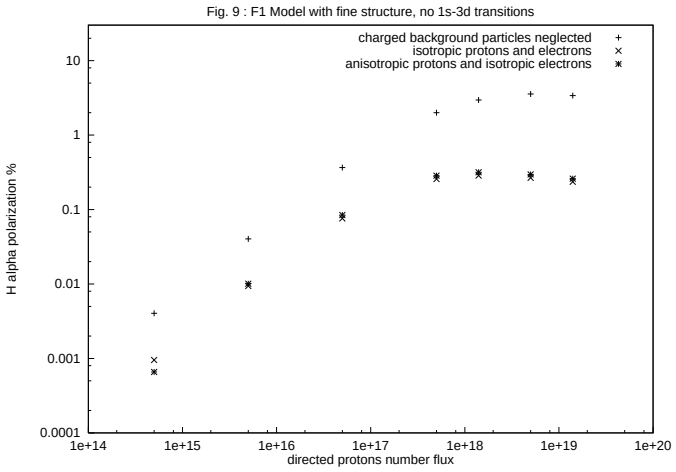

Fig. 9. See Fig. 1

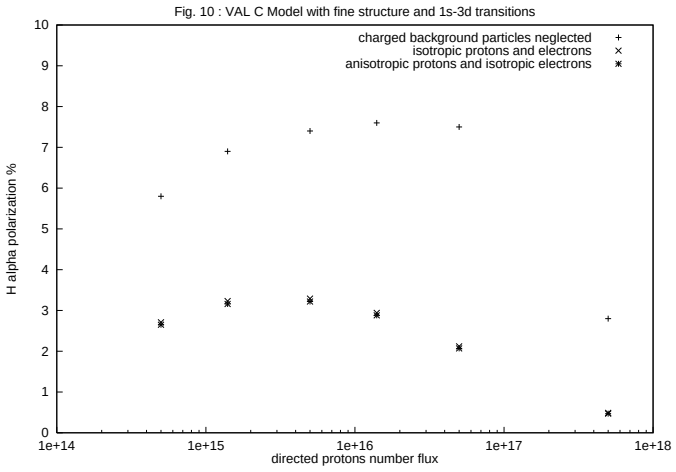

Fig. 10. See Fig. 1

by the collisions with the particles of the medium have a very significant depolarizing effect. For the H_α line, the depolarizing factor is of the order of two to four in the quiet atmosphere and of the order of ten in the flaring atmosphere where the electron and proton density is significantly higher.

A significant polarization degree can be obtained for the *VAL C* (between 2 and 6 %) and *VAL F* models (between 1 and 4 %). For both atmospheric models, the maximum of polarization degree corresponds to a proton number flux of $\mathscr{F}$ = 5 10^{15} cm^{-2}.s^{-1} (energy flux at injection site of $\mathscr{E}$ = 1.8 10^9 ergs.cm^{-2}.s^{-1}). This proton number flux is quite reasonable since it corresponds to a total energy in protons of the order of 10^{30} ergs (Assuming a flare surface of the order of 10^{18} cm^2 and a duration of the order of 10^3 s), whereas the typical energy in a big flare is of the order of 10^{32} ergs. It should be noted however that this proton flux does not cause a significant enhancement of the outcoming radiation field; in particular, the outcoming intensities in Ly_α and Ly_β are at least an order of magnitude below those given by the flare model *F1* without proton bombardment.

The polarization obtained when the solar atmosphere is represented by the flare model *F1* is significantly lower than in the previous ones. The maximum (between 0.3 and 1 %) is also obtained for a much higher value of the number flux of $\mathscr{F}$ = 1.4 10^{18} cm^{-2}.s^{-1} (energy flux at injection of $\mathscr{E}$ = 5 10^{11} ergs.cm^{-2}.s^{-1}). This comes from the fact that the local radiation field in this model is significantly higher than in the VAL ones and so a much higher proton flux is needed to saturate the impact polarization (as shown by the computations without background particles). The lower value of the maximum polarization obtained with background particles is due to the higher density of these particles in the flaring model (up to an order of magnitude). Such a high proton flux could be problematic as it corresponds to a total energy of the order of 5 10^{32} ergs (assuming the same mean surface and duration as previously). In particular, such high energy in accelerated protons should generate an observable flux in γ ray lines (the energy in protons above 1 MeV would be of the order of 10^{31} ergs). These are not observed for all the flares where H_α polarization has been seen. However, all the computations have been done assuming

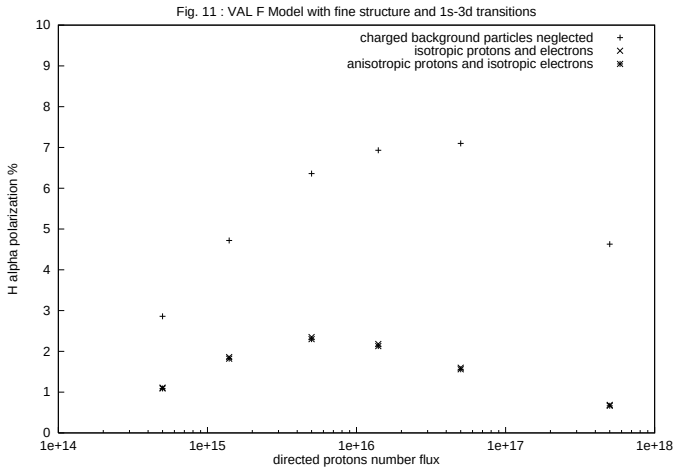

Fig. 11. See Fig. 1

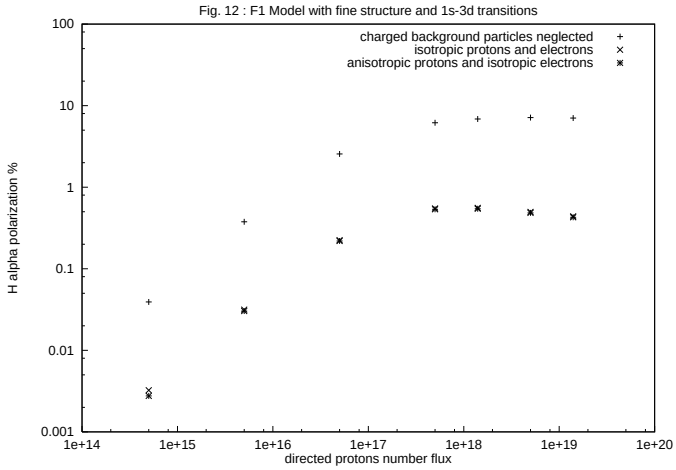

Fig. 12. See Fig. 1

a $\delta = 4$ value for the exponent of the protons power law spectrum. Increasing the value of this parameter would give a softer spectrum with a greater number of low energy protons relative to high energy ones. With a value of 6 for example, and the same number flux, the total energy above 1 MeV would be reduced to approximately 10^{29} ergs. Increasing the spectral index would have also the advantage of rising the polarization degree by rising the relative number of the lower energy protons that are the ones generating polarization parallel to the proton beam direction of propagation.

In a reported observation (Hénoux 1991), the observed polarization covers a wide area, close to 10^{19} cm^2, putting severe constraints on the energy budget if model F1 has to be used over all this area. As a matter of fact the region of high brightness requiring to use models like F1 does not cover the total 10^{19} cm^2 area where polarization is observed. This keeps the amount of energy needed to explain the observed polarization to values in the 10^{32} ergs range. However, a spectral index higher than 4 must be used in order to explain the lack of γ ray lines emission and we are close to the limit of what is acceptable in terms of energy budget (Fletcher 1997).

It still remains that the polarization degrees obtained here are somewhat smaller than the observed values: up to an order of magnitude if we compare the results obtained with the *F1* model and the observed polarization degrees of 5 to 10 percent. The results obtained for pre-flare conditions (VAL models) agree better with observations, but polarization is not only observed in the beginning of the flares.

6. Conclusion

So our computations show that a significant polarization is expected at the beginning of the flare or in regions in the flare that are not the brightest one. Indeed, some observations (still under work) suggest that the maximum of polarization is not always located at the brightest H_α pixels. If it is confirmed, it will be another argument in favour of the impact polarization theory.

Polarization does not increase linearly with the beam proton number flux since proton bombardment leads both to an increase of the Ly_α, Ly_β and H_α line intensities and of the background electrons and protons densities. These two processes are depolarizing. However, if the increase of the local electron and proton number densities is indeed a depolarizing factor, this may not be true for the radiation field. For simplicity, and since we were not able to treat fully the transfer of polarized radiation, the incident radiation field has been treated as unpolarized in the statistical equilibrium equations. Therefore, as shown by the analytical calculation of Ly_α polarization presented in appendix, a rise of the radiative terms in the statistical equilibrium equations severely decreases the resulting polarization when the radiation exciting the transition is originally supposed to be fully non polarized.

As a matter of fact, since the increase of the radiation field results from non-thermal anisotropic collisions leading to the emission of polarized photons, the assumption of zero polarization of the incoming radiation field is rather unrealistic. The natural continuation of our work is the coupling of polarized radiative transfer equations to statistical equilibrium equations to really follow the development of H_α polarization all along the flare evolution.

Acknowledgements. The authors wish to thank the referee for his pertinent comments and suggestions which helped us to improve this paper.

Appendix A: analytical solution of the statistical equilibrium equations for Ly$_\alpha$

In the simpler case of the Ly_α line, and without fine structure, it is easy to find an analytical solution for the polarization factor η, which is related to the polarization degree τ_{90} by Eq. (28).

Let us consider an hydrogen atom with 3 levels (1s, 2s, 2p) and without fine structure splitting. The physical processes to be taken into account are the following (Numerical values and notations are given in Table 4):

– Radiative excitation $1s \rightarrow 2p$ and deexcitation $2p \rightarrow 1s$.

Table 4. Statistical Equilibrium Equations Parameters for the **Ly**$_\alpha$ line. The numerical values are given for a directed proton number flux of 5 10^{15} cm^{-2}.s^{-1} in both models.

Parameter	Model VAL C	Model F1
Radiative processes		
$A(2p \rightarrow 1s) = A$	6.265 10^8 s^{-1}	6.265 10^8 s^{-1}
$B(1s \rightarrow 2p) I_{Ly_\alpha} = BI_\nu$	5.78 s^{-1}	1.55 10^3 s^{-1}
$B(2p \rightarrow 1s) I_{Ly_\alpha} = BI_\nu/3$	1.93 s^{-1}	5.17 10^2 s^{-1}
Non-thermal collisions		
${C^0}^{NT}(1s \rightarrow 2p) = C^{0NT}$	1.1 10^{-1} s^{-1}	1.1 10^{-1} s^{-1}
${C^2}^{NT}(1s \rightarrow 2p) = C^{2NT}$	-3.4 10^{-2} s^{-1}	-3.4 10^{-2} s^{-1}
Thermal collisions		
${C^0}^{th}(1s \rightarrow 2p) = {C^0}_{1s\rightarrow 2p}$	2.1 10^{-5} s^{-1}	3.6 10^{-2} s^{-1}
${C^2}^{th}(1s \rightarrow 2p) = {C^2}_{1s\rightarrow 2p}$	0 s^{-1}	0 s^{-1}
${C^0}^{th}(2p \rightarrow 1s) = {C^0}_{2p\rightarrow 1s}$	2.3 10^3 s^{-1}	1.5 10^4 s^{-1}
${C^2}^{th}(2p \rightarrow 1s) = {C^2}_{2p\rightarrow 1s}$	0 s^{-1}	0 s^{-1}
${C^0}^{th}(2s \rightarrow 2p) = N_P\alpha_0$	9.55 10^7 s^{-1}	6.62 10^8 s^{-1}
${C^2}^{th}(2s \rightarrow 2p) = N_P\alpha_2$	-5.94 10^6 s^{-1}	-3.42 10^7 s^{-1}
${C^0}^{th}(2p \rightarrow 2s) = N_P\frac{\alpha_0}{3}$	3.18 10^7 s^{-1}	2.21 10^8 s^{-1}
${C^2}^{th}(2p \rightarrow 2s) = N_P\frac{\alpha_2}{3}$	-1.98 10^6 s^{-1}	-1.14 10^7 s^{-1}

- Non-thermal collisions $1s \rightarrow 2p$ with directed protons (We neglect the non-thermal deexcitation $2p \rightarrow 1s$).
- Thermal collisions with the particles of the medium.

Following Eqs. (11), (13), (14), (18), (19), (15), (16) and (17); the statistical equilibrium equations are written as:

$$0 = -(BI_\nu + {C^0}_{1s\rightarrow 2p} + C^{0NT})\ {}^{1s}\rho^0_0 + 0\ {}^{2s}\rho^0_0 + \sqrt{3}(A + \frac{BI_\nu}{3} + {C^0}_{2p\rightarrow 1s})\ {}^{2p}\rho^0_0 + 0\ {}^{2p}\rho^2_0 \quad \text{(A1)}$$

$$0 = 0\ {}^{1s}\rho^0_0 + N_P\alpha_0\ {}^{2s}\rho^0_0 + \sqrt{3}N_P\frac{\alpha_0}{3}\ {}^{2p}\rho^0_0 + \frac{\sqrt{6}}{2}N_P\frac{\alpha_2}{3}\ {}^{2p}\rho^2_0 \quad \text{(A2)}$$

$$0 = \frac{1}{\sqrt{3}}(BI_\nu + {C^0}_{1s\rightarrow 2p} + C^{0NT})\ {}^{1s}\rho^0_0 + \frac{1}{\sqrt{3}}N_P\alpha_0\ {}^{2s}\rho^0_0 - (A + \frac{BI_\nu}{3} + {C^0}_{2p\rightarrow 1s} + N_P\frac{\alpha_0}{3})\ {}^{2p}\rho^0_0 - \frac{1}{\sqrt{2}}N_P\frac{\alpha_2}{3}\ {}^{2p}\rho^2_0 \quad \text{(A3)}$$

$$0 = \frac{1}{\sqrt{6}}{C^2}^{NT}\ {}^{1s}\rho^0_0 + \frac{1}{\sqrt{6}}N_P\alpha_2\ {}^{2s}\rho^0_0 - \frac{1}{\sqrt{2}}N_P\frac{\alpha_2}{3}\ {}^{2p}\rho^2_0 - (A + \frac{BI_\nu}{3} + {C^0}_{2p\rightarrow 1s} + N_P\frac{\alpha_0}{3} - N_P\frac{\alpha_2}{6})\ {}^{2p}\rho^2_0 \quad \text{(A4)}$$

These equations are clearly not independant: (A1) = $-$((A2) + $\sqrt{3}$(A3)). We can then suppress the first one and introduce $x_s = {}^{2s}\rho^0_0/{}^{1s}\rho^0_0$, $x_p = {}^{2p}\rho^0_0/{}^{1s}\rho^0_0$, $y_p = {}^{2p}\rho^2_0/{}^{1s}\rho^0_0$ to obtain:

$$0 = -\ N_P\alpha_0\ x_s + \frac{1}{\sqrt{3}}N_P\alpha_0\ x_p + N_P\frac{\alpha_2}{\sqrt{6}}\ y_p \quad \text{(A5)}$$

$$-\frac{1}{\sqrt{3}}(BI_\nu + {C^0}_{1s\rightarrow 2p} + C^{0NT}) = \frac{1}{\sqrt{3}}N_P\alpha_0\ x_s - (A + \frac{BI_\nu}{3} + {C^0}_{2p\rightarrow 1s} + N_P\frac{\alpha_0}{3})\ x_p - N_P\frac{\alpha_2}{3\sqrt{2}}\ y_p \quad \text{(A6)}$$

$$-\frac{C^{2NT}}{\sqrt{6}} = \frac{1}{\sqrt{6}}N_P\alpha_2\ x_s - N_P\frac{\alpha_2}{3\sqrt{2}}\ x_p - (A + \frac{BI_\nu}{3} + {C^0}_{2p\rightarrow 1s} + N_P\frac{\alpha_0}{3} - N_P\frac{\alpha_2}{6})\ y_p \quad \text{(A7)}$$

From these, we extract the following expressions for x_p and y_p:

$$x_p = \frac{1}{\sqrt{3}}\frac{BI_\nu + {C^0}_{1s\rightarrow 2p} + C^{0NT}}{A + \frac{BI_\nu}{3} + {C^0}_{2p\rightarrow 1s}} \quad \text{(A8)}$$

$$y_p = \frac{\frac{1}{\sqrt{6}}C^{2NT}}{A + \frac{BI_\nu}{3} + {C^0}_{2p\rightarrow 1s} + \frac{N_P\alpha_0}{6}(2 - x - x^2)} \quad \text{(A9)}$$

introducing $x = \frac{\alpha_2}{\alpha_0}$.

With Eq. (27), we deduce the expression of the polarization factor η:

$$\eta = \frac{1}{2\sqrt{2}}\frac{y_p}{x_p} = \frac{1}{4}\frac{C^{2NT}}{BI_\nu + {C^0}_{1s\rightarrow 2p} + C^{0NT}}\ \frac{1}{1+\tau_D} \quad \text{(A10)}$$

where τ_D is the depolarization rate by the particles of the medium:

$$\tau_D = \frac{\frac{N_P\alpha_0}{6}(2 - x - x^2)}{A + \frac{BI_\nu}{3} + {C^0}_{2p\rightarrow 1s}} \quad \text{(A11)}$$

These last two equations clearly show that the polarization is created by the anisotropic non-thermal collisions (${C^2}^{NT}$) and is destroyed by the incident radiation (BI_ν) and the isotropic collisions (${C^0}^{NT}$, ${C^0}_{1s\rightarrow 2p}$). The collisions with the particles of the medium always have a depolarizing effect (via $\tau_D > 0$), even if these particles have an anisotropic velocity distribution ($x \neq 0$). Such an anisotropy can modify the depolarization rate but is unable to raise the polarization to a higher value than the one created by the directed beam.

The results given by this analytical calculation for the Ly_α line with only the $n = 1$ and $n = 2$ levels and without fine

structure are practically identical to those we obtain with our numerical computations where the $n = 3$ level is taken into account (The resolution of the statistical equations with three main levels also give results for Ly_α and Ly_β, although only H_α results are presented in this paper). This suggests that we don't need to introduce the higher energy levels in the statistical equilibrium equations.

Without depolarizing collisions with the particles of the medium, the polarization is determined by the ratio between directed collisions and incident radiation. With the flare model, the incident radiation is dominant ($BI_\nu \gg C^{NT}$) and the Ly_α line polarization is very weak ($\tau_{90} = 0,013\%$) for an unpolarized incident radiation field. On the other hand, in the case of the quiet model, the non-thermal and radiative excitations are of the same order of magnitude and we obtain a significant polarization degree ($\tau_{90} = 3.5\%$).

References

J. Aboudharam, K. Berrington, J. Callaway, N. Feautrier, J. C. Hénoux, G. Peach and H. E. Saraph: 1992, *A&A*, 262, 302–307

K. Blum: 1981, *Density Matrix Theory and Applications*, Plenum Press, New York and London

V. Bommier and S. Sahal-Bréchot: 1982, *Solar Physics*, 78, 157–178

V. Bommier, J.L. Leroy and S. Sahal-Bréchot: 1986, *A&A*, 156, 79–89, 90–94

V. Bommier, E. Landi degl'Innocenti, J.L. Leroy, and S. Sahal-Bréchot: 1994, *Solar Physics* 154, 231

G. Chambe and J.C. Hénoux: 1979, *A&A*, 80, 123–129

A.G. Emslie: 1978, *Astrophys. J.*, 224, 241–246

A.G. Emslie and J.C. Hénoux: 1995, *Astrophys. J.*, 446, 371–376

C. Fang, J.C. Hénoux and W.Q. Gan: 1993, *A&A*, 274, 917

U. Fano: 1949, *J. Opt. Soc. Am.*, 39, 859

U. Fano: 1954, *Phys. Rev.*, 93, 121

U. Fano: 1957, *Rev. Mod. Phys.*, 29, 74

L. Fletcher: 1997, *private communication*

J.C. Hénoux, G. Chambe, D. Smith, D. Tamres, N. Feautrier, M. Rovira and S. Sahal-Bréchot: 1990, *Astrophys.J.Suppl.*, 73, 303–311

J.C. Hénoux: 1991, *Solar Polarimetry*, Proceedings of the 11th NSO/Sac Peak workshop

J.C. Hénoux, C. Fang and W.Q. Gan: 1993, *A&A*, 274, 923

W. Fritsch and C. D. Lin: 1983, *Physical Review A*, 27, 3361–3364

M.E. Machado, E.H. Avrett, J.E. Vernazza and R.W. Noyes: 1980, *Astrophys. J.*, 242, 336–351

M. J. Penn and J. R. Kuhn: 1995, *Astrophys. J.*, 441, L51–L54

S. Sahal-Bréchot: 1974, *A&A*, 36, 355

S. Sahal-Bréchot: 1977, *Astrophys. J.*, 213, 887–899

S. Sahal-Bréchot, E. Vogt, S. Thoraval and I. Diedhiou: 1996, *A&A*, 309, 317–334

O. Schöller, J. S. Briggs and R. M. Dreizler: 1986, *J. Phys. B*, 19, 2505–2517

J. O. Stenflo: 1982, *Solar Physics*, 80, 209–226

J. E. Vernezza, E. H. Avrett and R. Loeser: 1981, *Astrophys.J.Suppl.*, 45, 635

E. Vogt: 1992, *Etude de la polarisation de la raie H_α lors de l'éruption solaire du 20 Juin 1989*, D.E.A. probationary research report, Paris VII University

E. Vogt and J.C. Hénoux: 1996, *Solar Physics*, 164, 345–359

This article was processed by the author using Springer-Verlag LaTeX A&A style file *L-AA* version 3.